

Turbulence Models and Heat Transfer in Nozzle Flows

X.-L. Tong* and E. Luke†
Mississippi State University,
Mississippi State, Mississippi 39762

Nomenclature

a_1	=	Bradshaw constant, = 0.31
F_{sst}	=	shear stress transport blending function
k	=	turbulent kinetic energy
T_{wall}	=	wall temperature
T_0	=	temperature at nozzle inlet
ν_t	=	kinematic turbulent viscosity
Ω	=	mean flow vorticity magnitude
ω	=	specific turbulent dissipation rate

Introduction

SIGNIFICANT resources have been spent on creating accurate and robust turbulence models for flows with adverse pressure gradients. Capturing correct boundary-layer profiles under adverse pressure gradients is of particular importance to the accurate modeling of separated flows. In favorable pressure-gradient flows, small-scale features of boundary layers generally do not couple to larger-scale flow features such as flow separations. As a result, problems that can occur in regions of favorable pressure gradients are more difficult to spot in standard benchmarks. However, accurate modeling of such flows will be required for reliable predictions of surface heat fluxes or shear stresses. Here we investigate the performance of Menter's two equation shear-stress-transport (SST) turbulence model¹ for heat-transfer computation under strongly favorable pressure gradients found in choked nozzle flows (such as required in rocket nozzle analysis and design).

We have observed anomalous behavior of the SST turbulence model for strongly favorable pressure-gradient flows. We shall demonstrate the anomaly using an experimental choked nozzle problem published in the open literature.² The anomaly in the computed heat transfer appears to be caused by the shear-stress-transport correction term of Menter's model. By design, this term should be active in near-wall regions under adverse pressure gradients. However, it also appears to incorrectly become active under strongly favorable pressure-gradient conditions.

SST Turbulence Model

The SST turbulence model¹ is a two-equation turbulence model that combines the best aspects of several turbulence models. For example, the k - ω model of Wilcox³ has superior numerical stability to the standard k - ε model. However, because of a nonphysical dependency on freestream values of ω the model is not suitable for free-shear flows. To achieve the best of both models, Menter uses a smooth blending function that transitions from the application of the k - ω model in near-wall regions to the k - ε model in the wake and free-shear flow regions. The resulting baseline model, denoted BSL, provides a reasonable compromise between both models.

Menter noted that turbulence models that employ Bradshaw's assumption (whereby the shear stress is proportional to turbulent

kinetic energy) are generally better suited to capturing adverse pressure-gradient flows. Menter observes that this is as a result of the term correctly accounting for the transport of principle turbulent shear stress. Using this observation, Menter modifies the BSL eddy viscosity, defined by $\nu_t = k/\omega$, such that the turbulent viscosity is suitably limited by Bradshaw's turbulent viscosity, defined by $\nu_t = a_1 k/\Omega$. The resulting "limited" turbulent viscosity formulation is given by

$$\nu_t = \frac{a_1 k}{\max(a_1 \omega, \Omega F_{\text{sst}})} \quad (1)$$

where the blending function F_{sst} is a function that has a value between zero and one that disables the modification (i.e., goes to zero) in free-shear regions. This modification to the BSL model creates the SST model. The SST model is now widely used and has demonstrated good results on a wide range of flows under adverse pressure gradients. We observe that the SST correction given in Eq. (1) harms the performance of the model under conditions of strongly favorable pressure gradients found in choked nozzle flows.

Validation Case

To validate the model for strongly favorable pressure-gradient flows, we select the experimental data provided by Back et al.² Their paper documents an experimental investigation of convective heat transfer from accelerated turbulent boundary layers in a cooled converging-diverging nozzle. The geometry of the nozzle used in their investigation consisted of a throat diameter of 4.58 cm, a contraction-area ratio 7.75 to 1, an expansion-area ratio of 2.68 to 1, a convergent half-angle of 30 deg, and a divergent half-angle of 15 deg.

In the experiment, compressed air was heated by the internal combustion of methanol before it entered the cooled nozzle. The ratio of methanol-to-air mass flow rates was small enough so that the products of combustion could be treated as air. The convective heat transfer to the cooled wall was measured by arrays of thermocouples embedded along the nozzle wall. As reported in Back et al.,² measured heat-transfer coefficients were repeatable to within 2% both from measurements at different axial stations and among experimental runs.

Although many cases were measured in the experimental setup, we only consider case no. 262, as this is the only case for which both the heat fluxes and the measured wall temperatures have been published in the open literature. The wall temperatures for this case are found in a separate paper by Bartz.⁴ Case 262 conditions consist of air heated through methanol burners at a pressure of 5.17×10^5 Pa and a temperature of 843 K. This heated air flowed along a 45.7-cm-long cooled-approach section, whereby it entered the converging-diverging nozzle just described.

Related Results

The SST turbulence model has been validated for nozzle flows described by Back et al. in a technical report by Vieser et al.⁵ We also note that this validation case has been repeated in a recent validation of a compressible wall-law boundary condition.⁶ In both of these cases, it is found that the SST turbulence model accurately predicts the experimental heat-transfer coefficient, contrary to our findings. Our simulation setup differs in one important aspect: we used a prescribed wall temperature from the experimental measurements, whereas their validation used a fixed wall temperature given by $T_{\text{wall}} = 0.5T_0$. Based on the wall temperatures of case 262, this wall temperature is a good approximation of the mean wall temperature. However, the measured wall temperature varies over a range that exceeds 100 K, particularly in the critical throat region of the nozzle. We shall demonstrate that there is significant uncertainty introduced by this assumption. We also seek to show that because of this error the report of Vieser et al.⁵ incorrectly concludes that the SST model outperforms all other tested turbulence models for this case. Despite these concerns, we verify that our simulation code is able to duplicate their validation result using the same fixed wall temperature boundary condition.

Received 9 March 2004; revision received 4 August 2004; accepted for publication 4 August 2004. Copyright © 2004 by the American Institute of Aeronautics and Astronautics, Inc. All rights reserved. Copies of this paper may be made for personal or internal use, on condition that the copier pay the \$10.00 per-copy fee to the Copyright Clearance Center, Inc., 222 Rosewood Drive, Danvers, MA 01923; include the code 0001-1452/04 \$10.00 in correspondence with the CCC.

*Assistant Research Professor, Engineering Research Center.

†Assistant Professor, Department of Computer Science and Engineering. Member AIAA.

Simulation Preliminaries

For the results presented here we use a finite volume flow solver for generalized grids, known as CHEM. Details of the numerical formulation are presented in the CHEM user guide.⁷ This solver implements Spalart–Allmaras,⁸ $k-\omega$ (Ref. 3), BSL, and SST turbulence models.¹ We have simulated this case using all of the listed turbulence models, where the first three models produced similar results; the SST model produced markedly different results. For this presentation we will limit the discussion to the BSL and the SST model predictions as this is the most salient in the explanation of the difference in the SST model predictions.

For the thermodynamic properties of high-temperature air, we use a curve fit for γ that is fit to measured air properties from 300 to 850 K. Molecular viscosity and thermal conductivity were prescribed by Sutherland's law. We also note that we performed a grid-convergence study using three different grids. These grids ranged from 1) $151 \times 96 \times 2$, 2) $201 \times 79 \times 2$, and 3) $401 \times 115 \times 2$, where the finer grids were refined through the boundary layer as well as in the inviscid region. Because we are using a low-Reynolds-number model in the wall region, all grids had a $y^+ < 1$ for the first point off the wall. Numerical results for all grids varied at most a few percent. The results from grids 2 and 3 were identical establishing grid independence. The numerical results presented here are those computed on the finest ($401 \times 96 \times 2$) grid.

Simulation Results

To determine the effect of assuming a fixed wall temperature, we compare the SST turbulence model for case 262 using both a constant wall temperature of $T_{\text{wall}} = 0.5T_0$ and the prescribed experimental wall temperature. For this case we use a constant γ of 1.35 to match the assumptions of Vieser et al.⁵ Figure 1 shows the computed heat-transfer coefficients for both conditions. The throat of the nozzle is located at approximately 9.27 cm downstream of the nozzle inlet, and the peak in the heat-transfer coefficient occurs slightly before the throat. We note that the prescription of the actual experimental temperature lowers the peak computed heat-transfer coefficient by about 30%, quantifying the effect of using detailed experimental wall temperatures compared to prescribing an average fixed temperature. As can be seen and expected, heat fluxes have significant sensitivity to the prescribed wall temperature. We find as a result that the validation results of Vieser et al. for this case cannot be trusted, as the errors of this assumption alone are too significant for the case to be discriminatory.

We now perform a comparison of the BSL and SST turbulence models using the experimentally measured prescribed wall temperatures and a curve-fit γ for high-temperature air for case 262. The results of the simulations are shown in Fig. 2. Although the BSL model provides reasonably good agreement with the experimental data, the SST model predicts nearly a 20% lower peak heat transfer in the throat region. In addition, it appears that this lower heat transfer continues beyond the throat to the supersonic flow that follows.

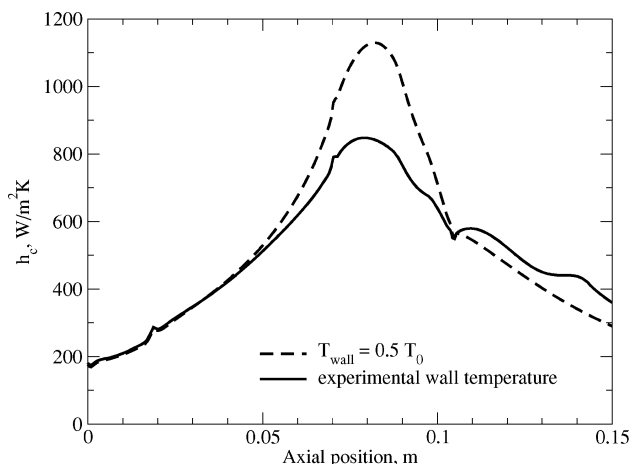


Fig. 1 Comparison of heat-transfer coefficients for different prescribed wall temperatures.

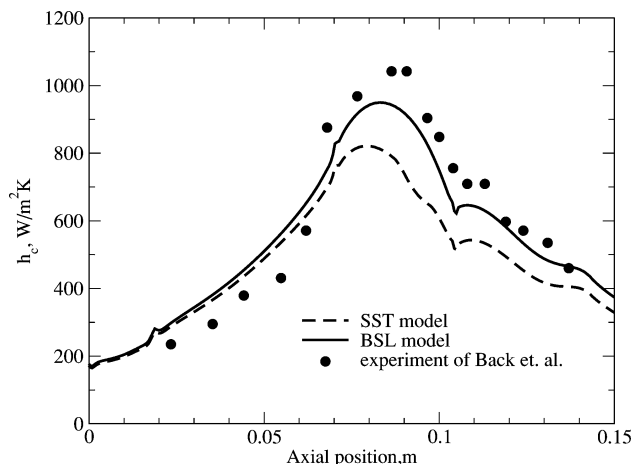


Fig. 2 Comparison of heat-transfer coefficients for BSL and SST models.

Comments on the SST Model Behavior

Why would the SST model produce different results from the BSL model? The main feature of the SST model that distinguishes it from the BSL model is the turbulent viscosity limiter given in Eq. (1), whereby the turbulent viscosity is limited to not exceed viscosity computed using Bradshaw's assumption. It is therefore reasonable to expect that the activation of this turbulent viscosity limiter would reduce the heat transfer. We have confirmed this by setting the blending function F_{sst} to zero and observing results consistent with the BSL model. Although this limiter dramatically improves the performance of the turbulence model in adverse pressure-gradient flows, it appears to be inappropriate in highly favorable pressure-gradient flows.

The turbulent viscosity defined by the SST model is essentially a heuristic correction to viscosity based on the observation that traditional two-equation eddy-viscosity models overpredict turbulent viscosity when turbulent energy production exceeds turbulent dissipation,¹ or when $\Omega > \omega$. The SST model transition between the standard two-equation eddy-viscosity model and Bradshaw's assumption occurs when $\Omega F_{\text{sst}} > a_1 \omega$. Because of the inclusion of Bradshaw's coefficient a_1 in this condition, the activation of the viscosity limiter occurs slightly before production exceeds dissipation. This slight adjustment of the activation point is justified by the need for continuity in the definition of turbulent viscosity. Sacrificing continuity, the correction can be applied only when production strictly exceeds dissipation, which results in a corrected turbulent viscosity of

$$\nu_t = \begin{cases} k/\omega & \text{if } \Omega F_{\text{sst}} \leq \omega \\ a_1 k / \Omega F_{\text{sst}} & \text{if } \Omega F_{\text{sst}} > \omega \end{cases} \quad (2)$$

This adjustment corrects the problem for the nozzle benchmark. Also, moving the switching point did not degrade the performance of the SST model on a sampling of adverse-pressure-gradient flow benchmarks. However, the discontinuity this fix introduces can frustrate numerical solvers. Continuity could be achieved by introducing an additional blending function perhaps based on the ratio of Ω and ω to provide a smooth transition. However, such an approach would also require the expense of recalibrating the model.

Conclusions

We have illustrated the importance of using experimental wall temperatures when performing heat-transfer validation work. In the specific example given here, the difference in the computed heat-transfer coefficient between using an average temperature and a specified temperature is about 30%. Once establishing an appropriate validation framework, we have identified a potential problem with the shear-stress-transport (SST) turbulence model. This problem is related to the model inappropriately applying Bradshaw's assumption in strongly favorable pressure-gradient conditions such as found in choked nozzle flows. As a result, we would recommend

disabling the SST model in these flow regions. However, we also suggest that it is possible to correct this shortcoming by slightly modifying the heuristic used to “turn on” the SST feature of the model. Extensive recalibration of the model by validating against a large body of cases would be required before such a modification should be trusted for general applications.

References

- ¹Menter, F. R., “Two-Equation Eddy-Viscosity Turbulence Models for Engineering Applications,” *AIAA Journal*, Vol. 32, No. 8, 1994, pp. 1598–1605.
- ²Back, L. H., Massier, P. F., and Gier, H. L., “Convective Heat Transfer in a Converging-Diverging Nozzle,” *International Journal of Heat and Mass Transfer*, Vol. 7, No. 5, 1964, pp. 549–568.
- ³Wilcox, D. C., “Reassessment of the Scale-Determining Equation for Advanced Turbulence Models,” *AIAA Journal*, Vol. 26, No. 11, 1988, pp. 1299–1310.
- ⁴Bartz, D. R., “Turbulent Boundary Layer Heat Transfer from Rapidly Accelerating Flow of Rocket Combustion Gases and of Heated Air,” edited by T. F. Irvine and J. P. Hartnett, *Advances in Heat Transfer*, Vol. 2, 1965, pp. 2–108.
- ⁵Vieser, W., Esch, T., and Menter, F., “Heat Transfer Predictions Using Advanced Two-Equation Turbulence Models,” CFX/ANSYS, Tech. Rept. CFX-VAL10/0602, Otterfing, Germany, June 2002.
- ⁶Nichols, R., and Nelson, C., “Wall Function Boundary Conditions Including Heat Transfer and Compressibility,” *AIAA Journal*, Vol. 42, No. 6, 2004, pp. 1107–1114.
- ⁷Luke, E. A., Tong, X.-L., Wu, J., and Cinnella, P., “CHEM 2: A Finite-Rate Viscous Chemistry Solver—The User Guide,” Mississippi State Univ., TR MSSU-COE-ERC-04-07, Mississippi State, MS, Sept. 2004.
- ⁸Spalart, P. R., and Allmaras, S. R., “A One-Equation Turbulence Model for Aerodynamic Flows,” *AIAA Paper* 92-0439, Jan. 1992.

P. Givi

Associate Editor

Impact of Compressibility on Mixing Downstream of Lobed Mixers

David E. Tew*

Massachusetts Institute of Technology,
Cambridge, Massachusetts 02139

James C. Hermanson†

Worcester Polytechnic Institute,
Worcester, Massachusetts 01609

and

Ian A. Waitz‡

Massachusetts Institute of Technology,
Cambridge, Massachusetts 02139

Introduction

LOBED mixers are used in a number of applications to augment the mixing rate between co-flowing fluid streams. These

devices enhance mixing by two mechanisms: the increased initial interface area associated with their convoluted trailing-edge shape and the introduction of streamwise vorticity.^{1–5} The focus of this Note is an assessment of the impact of compressibility on the mixing associated with streamwise vorticity.

In this work, the compressibility of the mixing layers is characterized by the convective Mach number M_c and the high-speed (primary) stream inflow Mach number M_P . The convective Mach number is defined as $M_c = (U_p - U_s)/\bar{a}$, where U_p is the high-speed (primary) stream velocity, U_s is the low-speed stream velocity, and \bar{a} is the mean inflow speed of sound. In planar shear layers, a threefold drop in the growth rate of planar shear layers has been observed⁶ as the convective Mach number increases from 0 to 1.

In lobed mixer flows with a supersonic high-speed stream, in addition to the mixer-generated vorticity, streamwise vorticity may be generated downstream of the mixer trailing edge via the interaction of trailing-edge shocks and density gradients across the mixing layer. Depending on the density ratio between the high-speed and low-speed streams, this baroclinic-torque-generated vorticity can either enhance or retard the mixing rate.

Description of Approach

The impact of compressibility on the streamwise-vorticity-enhanced mixing process was assessed in a series of wind-tunnel experiments and with the aid of a numerical discrete vortex model.

Experimental

The experiments were conducted in the Supersonic Shear Flow Facility at United Technologies Research Center.^{7,8} Two converging/diverging nozzles provided supersonic inflow Mach numbers of 1.3 or 2.4. A converging nozzle was used for the subsonic stream. The subsonic stream Mach number was varied by adjusting the inflow total pressure and mixing duct backpressure. The mixing duct was 10 by 10 cm in cross section and 64 cm long, and the inflow streams were of equal area. The two stream Mach numbers were varied in such a way that the velocity ratio remained constant, but the convective Mach number changed.

In addition to the compressibility of the mixing layers, the streamwise circulation shed from the trailing edge of the lobed mixers was independently controlled by the use of four different geometries: one planar splitter plate and three lobed mixers. Lobed mixers with either a 15- or a 25-deg ramp angle were designed to shed streamwise circulation; the third mixer was a convoluted plate with the same trailing-edge shape as the two lobed mixers but was not ramped and, therefore, shed little streamwise circulation. The mixers were of an approximately square lobe design with a height-to-wavelength ratio of $h^* = 1.25$. (The lobe wavelength was $\lambda = 0.31$ cm.) The nondimensional streamwise circulation shed by the two forced mixers were estimated by the scaling law developed by Barber et al.⁹:

$$\Gamma^* = \Gamma/\bar{U}h = 2 \tan \alpha \quad (1)$$

where Γ is the circulation, \bar{U} is the average inflow velocity of the two streams, h is the mixer height, and α is the ramp angle. The estimated nondimensional circulations for the 15- and 25-deg mixers were 0.5 and 0.9, respectively. The circulation shed by the convoluted plate mixer was estimated to be 0.1 based on Navier–Stokes computations performed by O’Sullivan⁴ for similar geometries.

The compressibility of the mixing layer as defined by the convective Mach number and primary Mach number was controlled by varying the inflow Mach numbers of the two streams. The convective Mach number ranged from 0.3 to 0.8 and the primary stream Mach number from 1.3 to 2.4.

The experimental diagnostics included schlieren photographs, Mie scattering imaging, and pitot/static pressure surveys. Mie scattering sites were provided by seeding the supersonic stream with methanol liquid upstream of the plenum chamber.¹⁰ Laser illumination was provided by a frequency-doubled Nd:YAG laser formed into a sheet roughly 5 cm wide and 1 mm thick. The planar Mie images were obtained with a charge-coupled device camera with an array of 576×384 pixels. The schlieren photographs and Mie images were used to develop a qualitative understanding of the mixing

Received 22 December 2001; accepted for publication 26 April 2002. Copyright © 2004 by the American Institute of Aeronautics and Astronautics, Inc. All rights reserved. Copies of this paper may be made for personal or internal use, on condition that the copier pay the \$10.00 per-copy fee to the Copyright Clearance Center, Inc., 222 Rosewood Drive, Danvers, MA 01923; include the code 0001-1452/04 \$10.00 in correspondence with the CCC.

*Graduate Research Assistant, Department of Aeronautics and Astronautics; currently Product Manager, UTC Fuel Cells, South Windsor, CT 06074; david.tew@utcfuelcells.com. Member AIAA.

†Associate Professor, Mechanical Engineering Department; currently Associate Professor, Department of Aeronautics and Astronautics, University of Washington, Seattle, WA 98195; jherm@aa.washington.edu. Associate Fellow AIAA.

‡Professor and Deputy Head, Department of Aeronautics and Astronautics; iaw@mit.edu. Associate Fellow AIAA.